EXPERIMENTAL AND NUMERICAL MODAL ANALYSIS OF COMPOSITE LAMINATED SHELLS WITH CUT-OUT

(DOI No. 10.3940/rina.ijme.2019.a1.495)

A Mandal, Narula Institute of Technology, India, **C Ray** and **S Haldar**, Indian Institute of Engineering Science and Technology Shibpur, India

SUMMARY

The presence of cutouts at different positions of laminated shell component in marine and aeronautical structures facilitate heat dissipation, undertaking maintenance, fitting auxiliary equipment, access ports for mechanical and electrical systems, damage inspection and also influences the dynamic behaviour of the structures. The aim of the present study is to establish a comprehensive perspective of dynamic behavior of laminated deep shells (length to radius of curvature ratio less than one) with cut-out by experiments and numerical simulation. The glass epoxy laminated composite shell has been prepared in the laboratory by resin infusion. The experimental free vibration analysis is carried out on laminated shells with and without cut-out. The mass matrix is developed by considering rotary inertia in a lumped mass model in the numerical modeling. The results obtained from numerical and experimental studies are compared for verification and the consistency between mode shapes is established by applying modal assurance criteria.

NOMENCLATURE

u, v, w	Displacements along x, y and z directions
θx, θy	Total rotations about y and x axis respectively
E1, E2 & E3	Modulus of elasticity along and transverse to fiber direction.
G12, G13 &G23	Rigidity moduli
v_{12}, v_{13} & v_{23}	Poisson's ratios
λ	fundamental frequency parameters
h	Thickness of the shell
a	Straight length of the shell in X direction
b	Straight length of the shell in Y direction
L	Curve length of the shell in Y direction
R	Radius of curvature of the shell
$\emptyset_x = \emptyset_y$	Average shear rotation throughout the thickness of laminated shell.
ω	Natural frequencies
λ	Non-dimensional natural frequencies
ρ	The density of the material

1. INTRODUCTION

In the construction of the ship hull, boats and other complex marine structures with lightweight requirement laminated composite shells (both shallow and deep) with their unique material properties as well as advantageous structural forms are preferably provided as primary structural components. The cut-outs in shells are necessary for heat dissipation, undertaking maintenance, fitting auxiliary equipment, access ports for mechanical and electrical systems, damage inspection of the structures etc. Presence of cut-outs affects the dynamic characteristics of the shells altering the resonant frequency. Henceforth, the study of dynamic behaviour of laminated shells with cut-outs becomes necessary to avoid induced acoustic noise, mechanical failure due to resonance and fatigue due to sustained vibrations. Shell structures offer superior performance in carrying loads and moments for combined bending and membrane action due to curved configuration. Multilayered composite materials have wide spread application in complicated structures for their unique material properties like high specific strength and ability to be tailored. The analysis of laminated composite structures has attracted several researchers since few decades. It has been improved day by day to achieve more realistic outcome. Various numerical investigations have been carried out on the vibration of composite shells using different techniques so far.

The initial attempts were made with Kirchoff's hypothesis where a number of problems were faced. The major problem concerned with the satisfaction of normal slope continuity at the element edges could not be solved satisfactorily by this. In the subsequent study, the above problem has been eliminated by adopting Mindlin's hypothesis where the effect of shear deformation has been considered. Reddy (Reddy, 1984) presented an extension of the Sanders shell theory to a shear deformation theory of laminated shells to find out exact solution of laminated shells under various kind of loading. A third-order theory of plates and shells had been presented by Reddy and Liu (Reddy & Liu, 1985). Bhimaraddi (Bhimaraddi, 1991) presented free vibration analysis of doubly curved laminated shells on rectangular plan form using three-dimensional elasticity theory. Sabir et al. (Sabir et al, 1994) used a strain-based finite element method to find out natural frequencies of cylindrical shells. The free vibration analysis of laminated composite shells with cutouts was presented by Chakravorty et al. (Chakravorty et al, 1998). Qatu (Qatu, 1999) used a modified rigidity matrix using FSDT to get more accurate results in terms of natural frequency for deep shell. Ganapathi and Haboussi (Ganapathi & Haboussi, 2003) studied free vibration of thick laminated anisotropic non-circular cylindrical shells. Qatu (Qatu, 2004) applied first-order shear deformation shell theory to study free vibration of laminated cylindrical and barrel thick shells. Djoudi and Bahai (Djoudi & Bahai, 2004) made a numerical investigation to find out the effect of cut-outs on the dynamic behaviour of cylindrical panels, using a strain based finite element method. Ganesan and Kadoli (Ganesan & Kadoli, 2004) worked on linear thermo elastic buckling and free vibration analysis of geometrically perfect hemispherical shells with cut-out using FSDT. Sheikh et al. (Sheikh et al., 2004) proposed a high precision shear flexible triangular element for vibration analysis of composite shell. Asadi et al. (Asadi et al., 2012) presented Static and vibration analyses of thick deep laminated cylindrical shells using 3D and various shear deformation theories. Pastor et al. (Pastor et al, 2012) presented a detail review on use of the modal assurance criteria. Malekzadeh et al. (Malekzadeh et al., 2013) carried out a three-dimensional free vibration analysis of functionally graded cylindrical panels with cut-out using Chebyshev–Ritz method. Kumar et al. (Kumar et al, 2014) worked on dynamic response of laminated composite shells using higher order zigzag theory. Li et al. (Li et al, 2014) introduced a direct method to calculate the sensitivity of MAC using a Lagrange function. Thakur and Ray (Thakur & Ray, 2015) studied the effect of thickness coordinate to radius of curvature ratio on free vibration of moderately thick and deep doubly curved cross-ply laminated shell.

Extensive literature review shows that the numerical analysis of laminated composite shallow shells has been carried out by several researchers. Whereas from reports on the dynamic analysis of deep shells it is clear that most of the researchers remained restricted up to length to radius of curvature ratio greater than or equal to one. Therefore there is a gap in this field in particular experimental modal analysis on laboratory made FRP shells with modal validation are scarce in the published literatures. Henceforth, experimental modal analysis along with numerical simulation of laminated shells with and without cutout has been carried out and presented in this paper to fill the gap in this field. The laminated shells have been prepared in the laboratory by resin infusion process using vacuum bagging and by maintaining a fixed fibre volume ratio and zero void content. In the finite element formulation, a lumped mass model is developed by considering the effect of rotary inertia (Mandal et al., 2017). The correlation of mode shapes between experimental and numerical data has also been identified in the present paper by using modal assurance criteria (MAC).

2. EXPERIMENTAL PROCESS AND DATA ACQUISITION

2.1 PREPARATION OF LAMINATED SHELLS

The laminated shells have been prepared in the laboratory within vacuum bag through resin infusion process as shown in Figure 1(a). The epoxy resin is selected as matrix material and bi-directional glass fabrics are chosen for the preparation of laminate as shown in Figure 1(b). The S-glass/epoxy (GFRP) laminated shell prepared in the laboratory is shown in Figure 1(c).

2.2 DETERMINATION OF MATERIAL PROPERTIES

2.2 (a) Elastic properties of laminated shell

The transducers along with associated instrumental set up of Olympus 45MG Ultrasonic thickness gage (UTG) and specialized high viscosity couplant or shear gel is used to measure longitudinal and shear wave sound velocities of the test specimens. The elastic properties viz. Modulus of elasticity (E), Poisson’s ratio (ν) and Shear modulus (G) are determined by non-destructive testing as per ASTM E494 – 10 (Liu et al, 2014). And the values are- E_1=30.4 GPa, E_2=30.4 GPa, E_3=9.95 GPa, ν_{12}=0.247, ν_{23}= ν_{13}=0.301, G_{12}=3.99 GPa,G_{23}= G_{13}=11.7 GPa and Density = 2064 Kg/m^3.

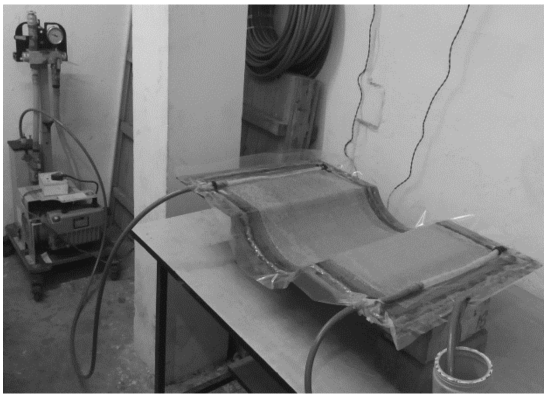

(a) Vacuum bagging technique

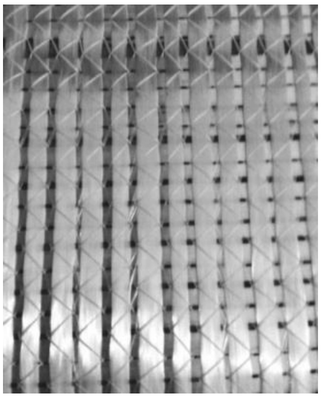

(b) Bi-directional glass fabrics

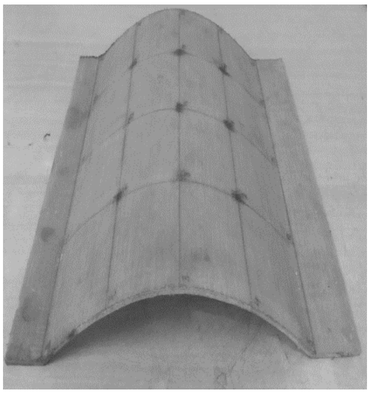

(c) Laminated GFRP shell

Figure 1

2.2 (b) Experimental modal analysis and data acquisition

The experimental study on the modal analysis of composite shells have been carried out using Bruel & Kjaer accelerometer (type- 4507). The accelerometer is placed on a pre-selected degree of freedom. An impact hammer (B & K type-8206) is used to provide impact at selected locations on the shell. The input and the output data are stored in a computer by means of a data acquisition system (B & K Photon plus) and RT pro modal analysis software with FFT (Fast Fourier Transform) analyzer. The experimental set up is shown in Figure. 2. The mode shapes are obtained by the post processing of acquired data from experimental data using pulse reflex software.

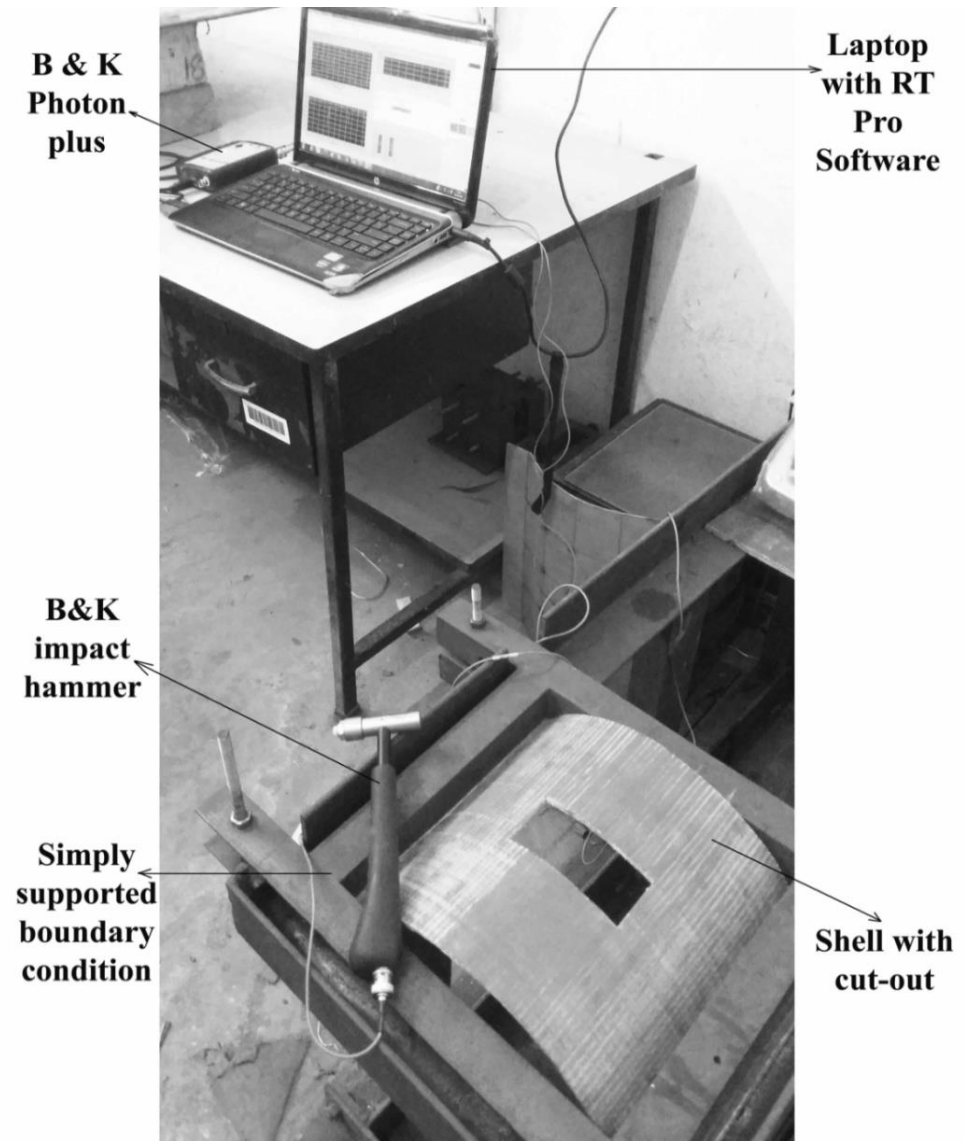

Figure 2: Experimental set up for Modal analysis

3. MATHEMATICAL FORMULATION

3.1 FINITE ELEMENT MODEL FOR MODAL ANALYSIS

The finite element model has been developed in the present study and a computer code is prepared using FOTRAN.

A nine noded isoparametric quadrilateral (four corner nodes, four mid side nodes and one at the centre of the element) shallow shell element (Mandal et al.,2017) with five degrees of freedom (u, v, w, θ_x and θ_y) at each node has been considered for the present formulation. The nodal displacement components at any node 'r' of the element can be written as:

$$\{\delta_r\}^T = \{u_r \quad v_r \quad w_r \quad \theta_{xr} \quad \theta_{xr}\} \tag{1}$$

where,

$$u = \sum_{r=1}^{9} N_r u_r, \quad v = \sum_{r=1}^{9} N_r v_r, \quad w = \sum_{r=1}^{9} N_r w_r,$$
$$\theta_x = \sum_{r=1}^{9} N_r \theta_{xr}, \quad \theta_y = \sum_{r=1}^{9} N_r \theta_{yr}$$

The shape functions N_r are developed by applying Lagrangian interpolation function. The effect of shear deformation can be expressed as the following, where the bending rotations are independent field variables.

$$\begin{Bmatrix} \emptyset_x \\ \emptyset_y \end{Bmatrix} = \begin{bmatrix} \theta_x - \frac{\partial w}{\partial x} \\ \theta y - \frac{\partial w}{\partial y} \end{bmatrix} \tag{2}$$

The constitutive relationship with respect to its reference plane may be expressed as

$$\{\sigma\} = [D]\{\varepsilon\} \tag{3}$$

Where, $\{\sigma\}$ is the stress resultants vector and can be expressed as-

$$\{\sigma\}^T = \begin{bmatrix} N_x & N_y & N_{xy} & M_x & M_y & M_{xy} & Q_x & Q_y \end{bmatrix} \tag{4}$$

And the strain vector can be expressed as

$$\{\varepsilon\}^T = \left[\left(\frac{\partial u}{\partial x} + \frac{w}{R}\right)\left(\frac{\partial v}{\partial y}\right) \quad \left(\frac{\partial u}{\partial y} + \frac{\partial v}{\partial x}\right) \quad -\frac{\partial \theta_x}{\partial x} \quad -\frac{\partial \theta_y}{\partial y} \quad - \left(\frac{\partial \theta_x}{\partial y} + \frac{\partial \theta_y}{\partial x}\right) \quad -\emptyset_x \quad -\emptyset_y\right] \tag{5}$$

Where, [D] is the rigidity matrix of laminated shell and written as

$$[D] = \begin{bmatrix} [A_{ij}]_{3\times3} & [B_{ij}]_{3\times3} & [0]_{3\times2} \\ [B_{ij}]_{3\times3} & [D_{ij}]_{3\times3} & [0]_{3\times2} \\ [0]_{2\times3} & [0]_{2\times3} & [A_{lk}]_{2\times2} \end{bmatrix} \tag{6}$$

where (A_{ij}), (B_{ij}), (D_{ij}) and (A_{lk}) are extensional, extension-bending coupling, bending and transverse shear stiffness matrices respectively and defined as

$$A_{ij} = \sum_{k=1}^{n} (Q_{ij})(z_k - z_{k-1}),$$
$$B_{ij} = \sum_{k=1}^{n} \frac{1}{2}(Q_{ij})(z_k^2 - z_{k-1}^2)$$
$$D_{ij} = \sum_{k=1}^{n} \frac{1}{3}(Q_{ij})(z_k^3 - Z_{k-1}^3)$$

where z_k is the distance of k^{th} layer from the reference plane.

The stiffness matrix $[K]_e$ of an element derived from the concept of virtual work method may be written as

$$[K]_e = \int_{-1}^{+1}\int_{-1}^{+1} [B]^T [D] [B] |J| \, d\varepsilon \, d\eta \tag{7}$$

where, [B] is the strain-displacement matrix and |J| is the determinant of Jacobian matrix. In the present formulation a consistent mass matrix having dimension 9x9 has been developed using the identical shape function used in Eq. 1 which may be expressed as

$$[M] = \rho h \iint [N]^T \, [N] \, dx \, dy \tag{8}$$

An element lumped mass matrix having dimension 45x45 has been developed using equation (8). The rotary inertia in the mass matrix has significant contribution to the dynamic behaviour of thicker laminates. Hence a lumped model of mass matrix has been derived including rotary inertia. The effect of rotary inertia has been examined by developing two types of proportionate mass lumping schemes. The effect of in-plane and transverse movements of mass has been considered in the first lumping schemes. This lumping scheme has been defined as 9NEWORI (mass lumping without rotary inertia) and may be expressed as

$$m_{ii}^{wl} = \frac{m_{ii}}{\sum m_{ii}} m_e$$

(i=1,2,3,6,7,8,11,12,13,16,17,18,21,22,23,26,27,28,31,32 ,33,36,37,38,41,42,43) (9)

where m_{ii}^{wl} are the i-th diagonal elements corresponding to u, v, w in the proposed model of lumped mass matrix, m_{ii} is the i-th diagonal element of the consistent mass matrix and m_e is the actual mass of element.

The mass lumping scheme considering the effect of rotary inertia (9NEWRI) along with in plane and transverse movement is expressed as.

$$m_{ii}^{wl} = \frac{m_{ii}}{\sum m_{ii}} m_e$$

(i=1,2,3,6,7,8,11,12,13,16,17,18,21,22,23,26,27,28,31,32 ,33,36,37,38,41,42,43) (10)

$$m_{ii}^{\theta xl} = \frac{h^2}{12}\frac{m_{ii}}{\sum m_{ii}} m_e \quad (i = 4,9,14,19,24,29,34,39,44) \tag{11}$$

$$m_{ii}^{\theta yl} = \frac{h^2}{12}\frac{m_{ii}}{\sum m_{ii}} m_e \quad (i=5,10,15,20,25,30,35,40,45) \tag{12}$$

The element stiffness and the mass matrices have been generated and assembled together to form the global stiffness matrix $[K_0]$ and the global mass matrix $[M_0]$. The equation of motion for the free vibration analysis is expressed as

$$[K_0]\{\delta\} = \omega^2[M_0]\{\delta\} \tag{13}$$

Eq.(13) is solved by using the simultaneous iterative technique following (Corr & Jenings, 1976) to compute the natural frequencies.

3.2 MODAL ASSURANCE CRITERION (MAC)

The modal assurance criteria have been determined to identify the degree of consistency between mode shapes obtained from experimental and numerical models. MAC is determined as a normalised scalar product of two sets of vectors $\{\emptyset_i\}$, $\{\Psi_j\}$. The resulting scalars are set into the MAC matrix-

$$MAC\ (i,j)\ = \frac{|\{\emptyset_i\}\{\Psi_j\}^T|^2}{(\{\emptyset_i\}\{\emptyset_i\}^T)\left(\{\Psi_j\}\{\Psi_j\}^T\right)} \tag{14}$$

$\{\emptyset_i\}$= Modal displacement vector from experimental data

$\{\Psi_j\}$ = Modal displacement vector of compatible mode from numerical analysis.

$\{\emptyset_i\}^T$ = Transpose of $\{\emptyset i\}$

$\{\Psi_j\}^T$=Transpose of $\{\Psi_j\}$

The numerical value of modal assurance criteria ranges between 0 to 1.The range of MAC 0.9 to 1.0 indicates that mode shapes from numerical and experimental data are greatly correlated and almost identical. The values less than 0.1 represent no correlation.

4. RESULTS AND DISCUSSIONS

4.1 VALIDATION OF THE PRESENT FINITE ELEMENT FORMULATION

Several numerical examples are solved and the results compared with published results to validate the present research work. The convergence is verified and the effect of rotary inertia in mass matrix has been studied.

4.1(a) Laminated cross-ply cylindrical shell panel with different thickness ratio (h/a)

A Simply supported laminated cylindrical shallow shell with varying thickness ratio (h/a) and curvature ratio (R/a) and lay-up sequence (0°/90°/0°) has been analysed in the present study. The material properties considered are E_1/E_2= 25, G_{12}=G_{13}=0.5E_2, G_{23}=0.2E_2, γ_{12} = 0.25. Non-dimensional fundamental frequency parameters $\lambda = \omega a^2\sqrt{(\rho\ /E_2)}/h$ obtained from both the mass lumping schemes are presented in Table 1 and compared with those obtained from the closed form solution in (Reddy, 1984). Table 1 shows a good agreement of present results with published literature and excellent convergence is established at different mesh divisions. It also shows that the mass lumping scheme with rotary inertia (9NEWRI) provides a better result than that obtained from 9NEWORI and the effect of rotary inertia becomes more prominent with the increase of thickness of the shell. So it can be observed from the results presented in the Table 1 that the effect of rotary inertia increases with the increase of thickness ratio(h/a) and 9NEWRI is more applicable for any kind of shell, therefore in further study we take only 9NEWRI under consideration.

4.1(b) Simply supported cross ply laminated cylindrical shell

Non-dimensional fundamental frequencies of simply supported cross-ply (0°/90°) laminated cylindrical shell panels with thickness ratio (a/h =10) have been evaluated using the present formulation with different (R/a) ratio. The material properties are considered as E_1/E_2= 25, G_{12}=G_{13}=0.5E_2, G_{23}=0.2E_2, γ_{12} = 0.25. Non-dimensional fundamental frequency parameters $\lambda = \omega a^2\sqrt{(\rho\ /E_2)}/h$ obtained from the present formulation are shown in Table 2 and compared with those obtained from FSDT, HSDT and three dimensional elasticity solution in (Bhimaraddi, 1991). It is observed from Table 2 that the present results are in very good agreement with published results. It is clearly observed from Table 2 that the present formulation is applicable for both shallow ($R/a > 2$) and deep ($R/a \leq 2$) shells.

4.1(c) Cross ply $(0°/90°)_4$ laminated cylindrical shallow shell with cut-out

Non-dimensional fundamental frequency of simply supported and fixed along all the four edges cross-ply $(0°/90°)_4$ laminated cylindrical shallow shell panel with central square cut outs having thickness ratio a/h =100 has been evaluated using the present formulation. The material properties are E_1/E_2= 25, G_{12}=G_{13}=0.5E_2, G_{23}=0.2E_2, γ_{12} = 0.25. Non-dimensional fundamental frequency parameters $\lambda = \omega a^2\sqrt{(\rho/E_2)}/h$ obtained from the present formulation are shown in Table 3 and compared with those obtained from FEM solution in (Chakravorty et al., 1998). It is observed from Table 4 that the present results are in very good agreement with the published results.

Table 1. Non-dimensional fundamental frequency of laminated cross-ply (0°/90°/0°) cylindrical shell, $\lambda = (\omega a^2/h)\sqrt{(\rho/E_2)}$ $(a = L, R_x = R, R_y = inf)$ (shown in Figure. 3)

R/a	h/a	(Reddy,1984)	Present Results		
			Mass lumping Schemes	Mesh division	Results
4	0.1	12.233	9NEWORI	8 X 8	12.5533
				12 x 12	12.5535
				16 x 16	12.5535
				20 x 20	12.5536
			9NEWRI	8 X 8	12.2703
				12 x 12	12.2705
				16 x 16	12.2706
				20 x 20	12.2706
4	0.01	22.709	9NEWORI	8 X 8	22.6915
				12 x 12	22.6925
				16 x 16	22.6927
				20 x 20	22.6927
			9NEWRI	8 X 8	22.7079
				12 x 12	22.7089
				16 x 16	22.7090
				20 x 20	22.7090
2	0.1	12.438	9NEWORI	8 X 8	12.8498
				12 x 12	12.8501
				16 x 16	12.8501
				20 x 20	12.8502
			9NEWRI	8 X 8	12.7888
				12 x 12	12.7892
				16 x 16	12.7892
				20 x 20	12.7892
2	0.01	36.77	9NEWORI	8 X 8	36.6348
				12 x 12	36.6369
				16 x 16	36.6372
				20 x 20	36.6382
			9NEWRI	8 X 8	36.6319
				12 x 12	36.6339
				16 x 16	36.6343
				20 x 20	36.6353

Table 2. Non-dimensional fundamental frequency of laminated cross-ply cylindrical shell, $\lambda = (\omega a^2/h)\sqrt{(\rho/E_2)}$ ($a = L$, a/h =10, $R_x = R$, R_y =inf) (shown in Figure. 3)

R/a	(Bhimaraddi, 1991)			Present Results [9NEWRI]
	3-D	FSDT	HSDT	
1	10.4085	10.7475	10.9189	10.3972
2	9.3627	9.3653	9.5664	9.3315
3	9.1442	9.0563	9.2642	9.0830
4	9.0613	8.9403	9.1506	8.9943

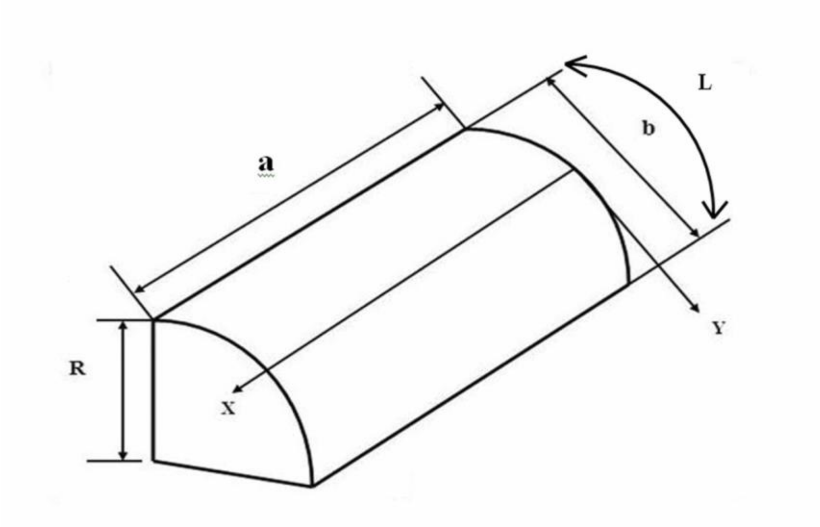

Figure 3: Line diagram of a shell

Table 3. Non-dimensional fundamental frequency of laminated cross-ply cylindrical shallow shell, $\lambda = (\omega a^2/h)\sqrt{(\rho/E_2)}$ ($a = b$, $a/h = 100$, $h/R_x = 1/300$, $R_y = inf$, $R_x = R$) (shown in Figure. 3)

Cut-out size (X- direction)	Cut-out size (Y- direction)	Simply supported		Clamped	
		(Chakravorty et al., 1998)	9NEWRI	(Chakravorty et al., 1998)	9NEWRI
0.1a	0.1b	27.042	27.212	68.776	69.128
0.3a	0.3b	27.913	28.067	59.317	59.638
0.5a	0.5b	29.472	29.3681	72.133	71.568

Table 4: Natural frequencies of a bidirectional laminated deep shell with a square cut-out at the centre and two curve edges free and other two straight edges simply supported (Only θ_y free)

Cut out size (X- direction)	Cut out size (Y- direction)	References	Mode 1	2	3
Without cut-out	Without cut-out	9NEWRI	290.68	663.19	668.95
		Experimental	285.209	638.347	643.211
		% Deviation	1.882	3.746	3.848
0.2a	0.2b	9NEWRI	285.247	670.03	670.09
		Experimental	271.586	655.373	669.061
		% Deviation	4.789	2.188	0.154
0.4a	0.4b	9NEWRI	255.676	410.937	593.22
		Experimental	255.348	413.796	555.854
		% Deviation	0.128	0.696	6.299
0.6a	0.6b	9NEWRI	239.863	303.331	387.487
		Experimental	242.97	302.132	388.376
		% Deviation	1.295	0.395	0.229
0.2a	0.4b	9NEWRI	280.93	526.226	665.34
		Experimental	272.292	521.803	672.93
		% Deviation	3.075	0.841	1.141
0.4a	0.6b	9NEWRI	267.861	326.677	540.063
		Experimental	261.187	325.978	544.256
		% Deviation	2.492	0.214	0.776

4.2 PRESENT INVESTIGATION AND EXPERIMENTAL VERIFICATION

The experimental verification of the present formulation has been carried out in the present study. The glass fibre reinforced composite laminates cylindrical shell consisting of 6 layers of bidirectional S glass fabric with average thickness 3mm and with plan size 245mm × 245mm have been fabricated in the laboratory. The radious of curvature of the shell is 145mm.The material properties of s-glass/epoxy laminate are determined in the laboratory through the non destructive testing method. The material properties obtained by using the ultrasonic thickness gauge as per ASTME 494-10 are presented at section 2.2(a).

4.2(a) Laminated shell panel with a square cut-out at centre

The natural frequencies and the corresponding mode shapes of laminated shells (with plan size 245mm × 245mm) with different size of square and rectangular (in plan) cut-out have been determined by experimental procedure as well as by numerical analysis. The natural frequencies for first three modes of a bidirectional s-glass/epoxy shell laminates with varying cut-out size (square and rectangular) are presented in Table 4. The curved edges of laminates are free and other two straight edges are simply supported (only θ_y is free). It is observed from Table 4 that the for shell with square cut-out fundamental frequencies decrease with the increase in the cut-out size, the reduction of mass being significant in this case. Other two natural frequencies increase first then decrease with the increase of the cut-out size. From the Table 4, it is also seen that natural frequency also depends on the shape (square and rectangular) of the cut outs. The corresponding sample mode shapes determined from experimental and numerical methods are presented in Figure 4 which shows a good resemblance with each other.

4.2(b) Consistency between numerical and experimental mode shapes by modal assurance criteria (MAC)

The modal assurance criteria (MAC) computed and presented in Table 5 to identify the correlation between the mode shapes obtained from experimental and numerical data for a deep shell with cut-out (0.4a × 0.6b) at center (presented in Figure.4). The degree of correlation between the mode shapes is indicated by the numerical values between 0 and 1.0. The values with bold letters represent mode to mode correspondence of MAC values. The numerical values (in bold) for first mode shape is very close to 1 which indicates an excellent correlation. Other two values (in bold) in MAC matrix are varying from 0.75 to 0.9 which indicate a good correlation between mode shapes obtained from experiment and numerical analysis.

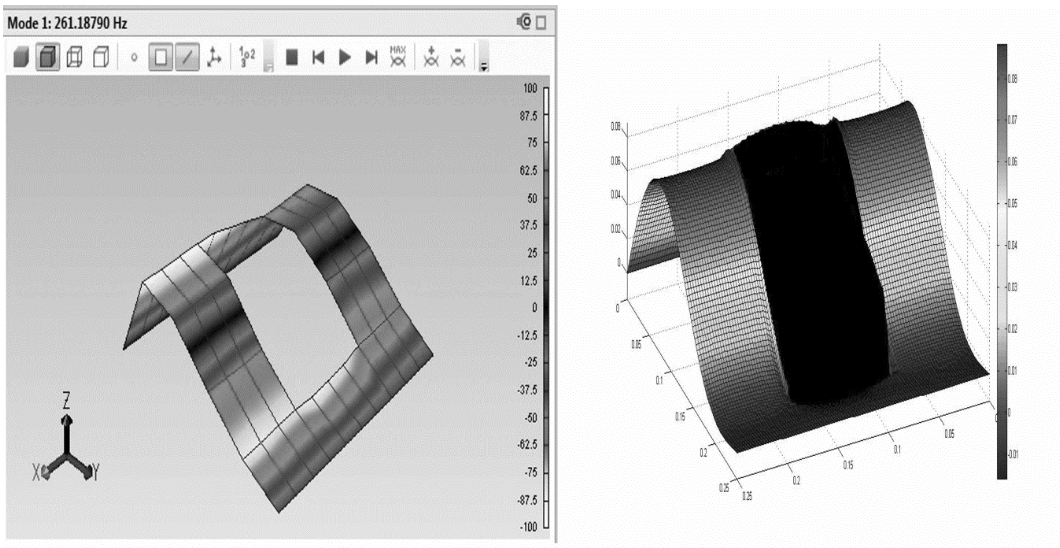

(a) (b)

(i) Mode shapes for 1st mode (a) Experimental (b) Numerical

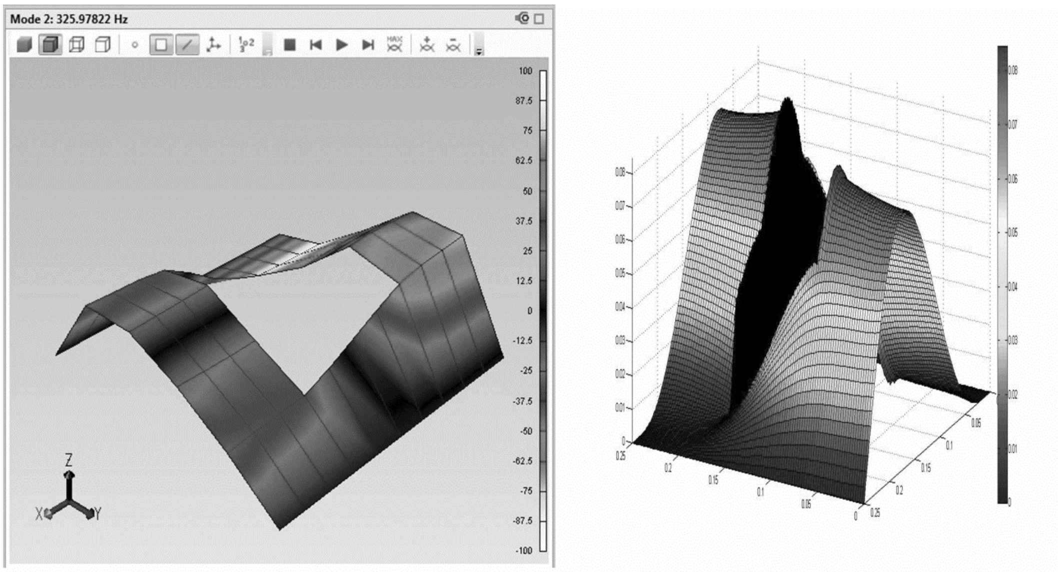

(a) **(b)**

(ii) Mode shapes for 2^{nd} mode (a) Experimental (b) Numerical

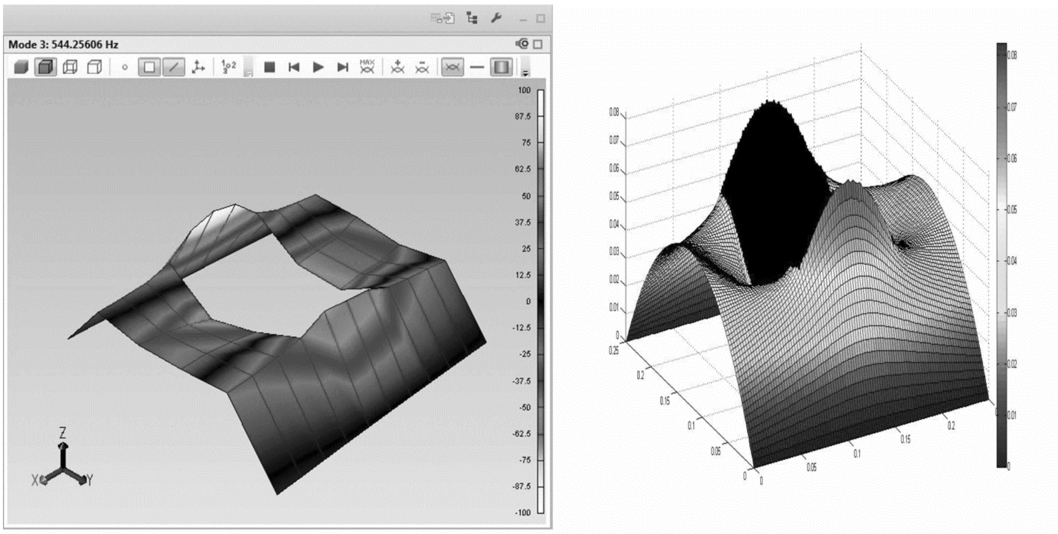

(a) **(b)**

(iii) Mode shapes for 3^{rd} mode (a) Experimental (b) Numerical

Figure 4: Mode shapes of a FRP deep shell with cut-out ratio: 0.4× 0.6

Table 5: MAC matrix for comparison of experimental and numerical mode shapes

Modal Frequency	Experimental	261.187	325.978	544.256
	267.861	***0.9708***	0.8548	0.5791
Numerical	326.677	0.9482	***0.8208***	0.5782
	544.256	0.8311	0.6312	***0.7666***

4.2(c) Effect of boundary condition and position of cut-out

To find out the effect of the boundary condition and the position of the cut-out, the bidirectional s-glass epoxy laminated cylindrical shell (plan size 245mm × 245mm and R=145mm) with a cut-out (0.2a ×0.2b) has been taken under consideration. The material properties used here is same as those are presented at section 2.2(a). The modal analysis has been done for all edges fixed and all edges simply supported boundary condition.

From the Figure 5 it is clear that natural frequencies vary with boundary condition. Changes of stiffness become significant there.

To observe the effect of position of the cut-out, the cut-out has been sifted gradually towards the support. For the first case cut-out has been shifted towards the support of the curve edge and in the next case the cut-out has been shifted towards the support of the straight edge of the shell. The effect of the position of the cut-out is plotted in Figure 5. It can be observed from Figure 5 that natural frequencies of the laminates change with the increasing distance of cut-outs from the centre of the shell. Figure 5(a) shows fundamental frequencies decrease with decreasing distance of the cut-out from the support of curved sides of the laminate. But when the cut-out is shifted towards the support of the straight side of the shell frequencies decrease initially and increase thereafter with the increment of the distance between cut-out and centre of the shell for both simply supported and fixed laminates. In the study of 2nd mode shape from Figure 5(b) it can be noticed that for fixed supported shell, fundamental frequencies increase initially and decrease thereafter with the increment of the distance of cut-out from shell centre, but the graphs show fully reverse pattern for simply supported laminates. For the 3rd mode from Figure 5(c) it can be observed that frequencies decrease initially and increase thereafter with the increment of the distance between cut-out and shell centre for both simply supported and fixed laminates. When cut-out is shifted towards the curved boundary, the plan area of the cut-out remains same. Whereas plan area reduces when cut-out is shifted towards straight edges resulting in the variation of stiffness of the shell. Although actual area of cut-out remains same, natural frequencies change due to the variation of stiffness of the shell.

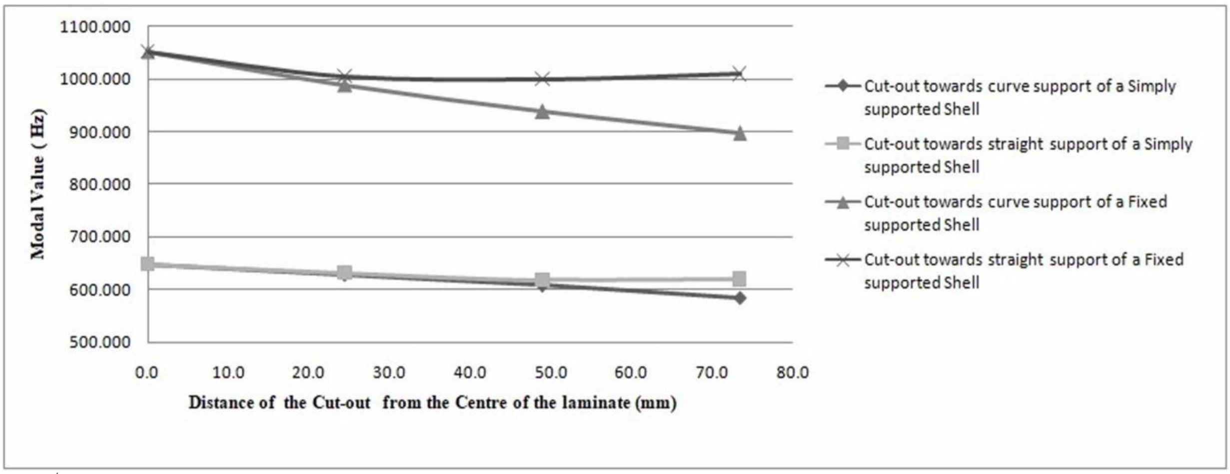

(a) 1st Mode

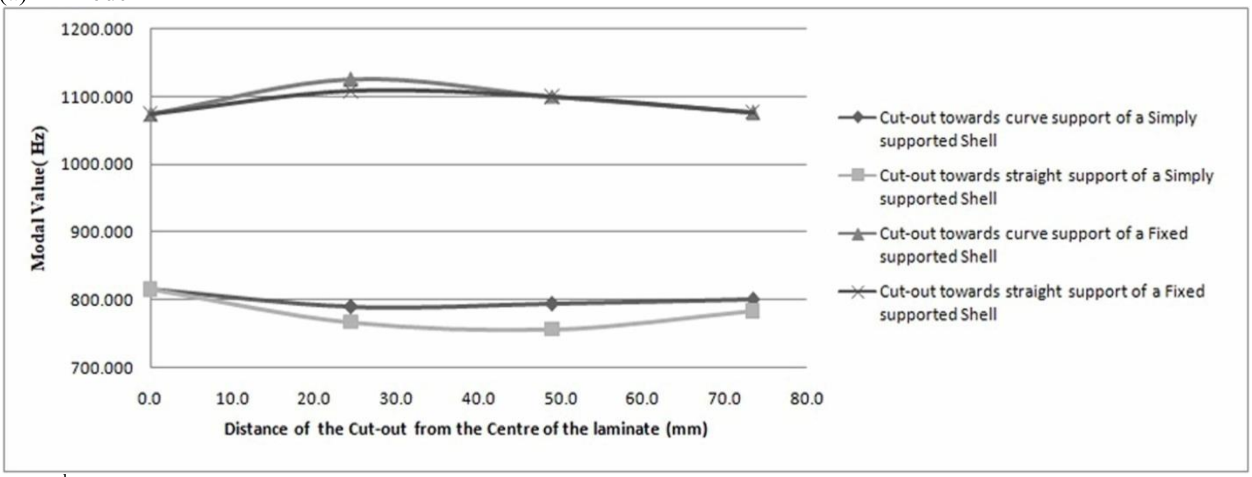

(b) 2nd Mode

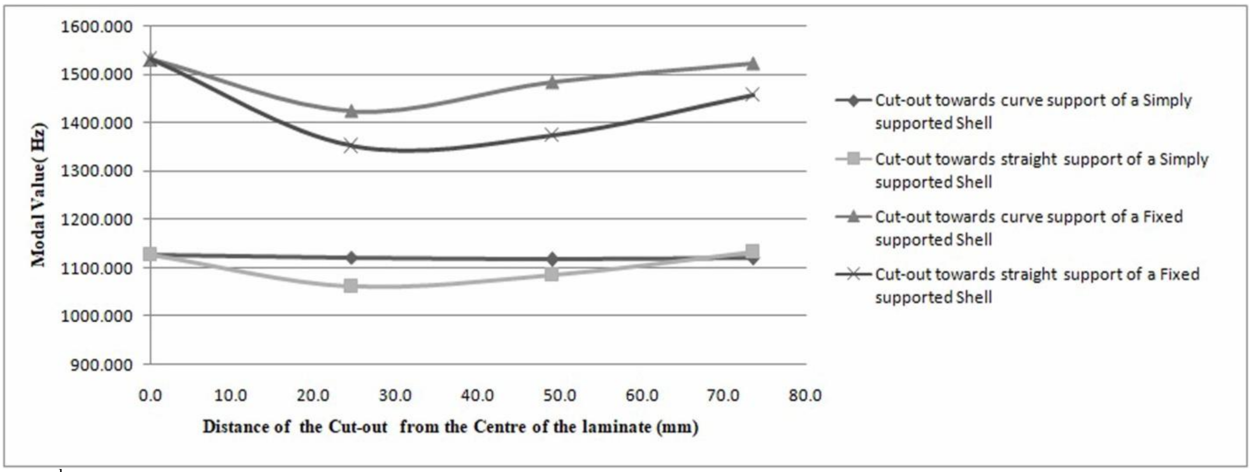

(c) 3rd Mode

Figure 5: Natural frequencies vs. Increasing distance of eccentric cut-outs from the centre of the shell

5. CONCLUSION

Numerical and experimental investigations have been carried out on bi-directional s-glass epoxy laminated shells with and without cut-out in the present study. The laminated shells have been prepared in the laboratory using vacuum bagging technique. It is observed that the variation of experimental results with those obtained from the present finite element analysis has never been exceeded 7% and that is quite reasonable. It is observed that there is a significant effect of rotary inertia on the free vibration of thick laminated shells. The mass lumping scheme with rotary inertia is suitable for both thick and thin shells whereas the mass lumping scheme without rotary inertia is suitable for thin shells only. It is clearly observed from the results in terms of natural frequencies for shells with cut-out that the natural frequency changes with the size of cut-out.

However natural frequencies of shells with rectangular and square cut-out show that the frequencies not only vary with the area of cut-out but also the shape of cut-out. Numerical and experimental results show that the boundary conditions of shells too have a major influence on the natural frequencies. It is noticed that the location of the cut-out also a large factor. In present analysis above 16% variation in fundamental frequencies can be observed for different positioning of the same size internal cut-out. The correlation between experimental and numerical outcome in terms of mode shape is also established through the numerical values of modal assurance criteria.

6. REFERENCES

1. REDDY, J.N. (1984) 'Exact solutions of moderately thick laminated shells', *Journal of Engineering Mechanics*, ASCE. 110.
2. REDDY, J.N. and LIU, C.F. (1985) 'A higher-order shear deformation theory of laminated elastic shells', *International Journal of Engineering Science*, 23, pp. 319–330.
3. BHIMARADDI, A.(1991)'Free vibration analysis of doubly curved shallow shells on rectangular planform using three-dimensional elasticity theory', *International Journal Solids Structures*, 27, pp.897–913.
4. SABIR, A.B., SFENDJI, A. and HUGHES, T.G. (1994) 'Strain based finite element for the natural frequencies of cylindrical shells', *Thin-Walled Structures*, 18 (1), 67-82.
5. CHAKRAVORTY, D., SINHA, P. K. and BANDYOPADHYAY, J.N. (1998) 'Applications of FEM on free and forced vibration of laminated shells', *Journal of Engineering Mechanics*, 124, pp.1-8.
6. QATU, M.S (1999) 'Accurate equations for laminated composite deep thick shells', *International Journal Solids Structures*, 36, pp.2917–2941.
7. GANAPATHI, M. and HABOUSSI, M. (2003) 'Free vibrations of thick laminated anisotropic non-circular cylindrical shells', *Composite Structures*, 60, pp. 125-133.
8. QATU, M.S., (2004) 'Theory and vibration analysis of laminated barrel thick shells', *Journal of Vibration and Control*, 10, pp.319-341. DOI: 10.1016/ s0020-7683 (98) 00134-6.
9. DJOUDI, M.S. and BAHA, I H. (2004) 'Strain based finite element for the vibration of cylindrical panels with openings', *Thin-Walled Structures*, 42(4), pp.575-588.
10. GANESAN, N. and KADOLI R, (2004)'Studies on linear thermo elastic buckling and free vibration analysis of geometrically perfect hemispherical shells with cut-out', *Journal of Sound and Vibration*, 277, pp.855-879.

11. SHEIKH A.H, HALDAR S and SENGUPTA D (2004) 'A high precision shear flexible triangular element for vibration of composite shell', *shock and vibration*, 11, pp.585-596.
12. ASADI A, WANG W and QATU M.S (2012) 'Static and vibration analyses of thick deep laminated cylindrical shells using 3D and various shear deformation theories', *Composite Structures*, 94(2), pp.494-500.
13. PASTOR, M., BINDA, M. and HARCARIK, T.(2012) 'Modal Assurance Criterion', Procedia Engineering, 48, pp. 543 – 548.
14. MALEKZADEH, P., BAHRANIFARD, F., and ZIAEE,S. (2013) 'Three dimensional free vibration analysis of functionally graded cylindrical panels with cut-out using Chebyshev – Ritz method', *Structures*, 105, pp. 1-13.
15. KUMAR, A., CHAKRABARTI, A. and P. BHARGAVA (2014) 'Accurate dynamic response of laminated composites and sandwich shells using higher order zigzag theory', *Thin-Walled Structures*, 77, pp.174-186.
16. LI, L., HU, Y. AND WANG, X. (2014) 'Direct way of computing the variability of modal assurance criteria', *Mechanics Research Communications,* 55, pp.53– 58.
17. S. N. THAKUR and C. RAY, (2015) 'The effect of thickness coordinate to radius ratio on free vibration of moderately thick and deep doubly curved cross-ply laminated shell', *Archive of Applied Mechanics*, 86(6),pp.1119–1132. DOI-https://doi.org/10.1007/s00419-015-1082-8.
18. MANDAL, A., RAY, C. AND HALDAR, S. (2017) 'Free vibration analysis of laminated composite skew plates with cut-out', *Archive of Applied Mechanics*, 87 (9), pp. 1511-1523.
19. ASTM E494(2010) Standard Practice for Measuring Ultrasonic Velocity in Materials.
20. CORR R.B and A JENNINGS, (1976) 'A simultaneous iteration algorithm for symmetric eigen value problems', *International Journal for Numerical and Engineering*, 10 ,pp.647-663.

